iScience

CellPress
OPEN ACCESS

Article

Zinc Dynamics during *Drosophila* Oocyte Maturation and Egg Activation

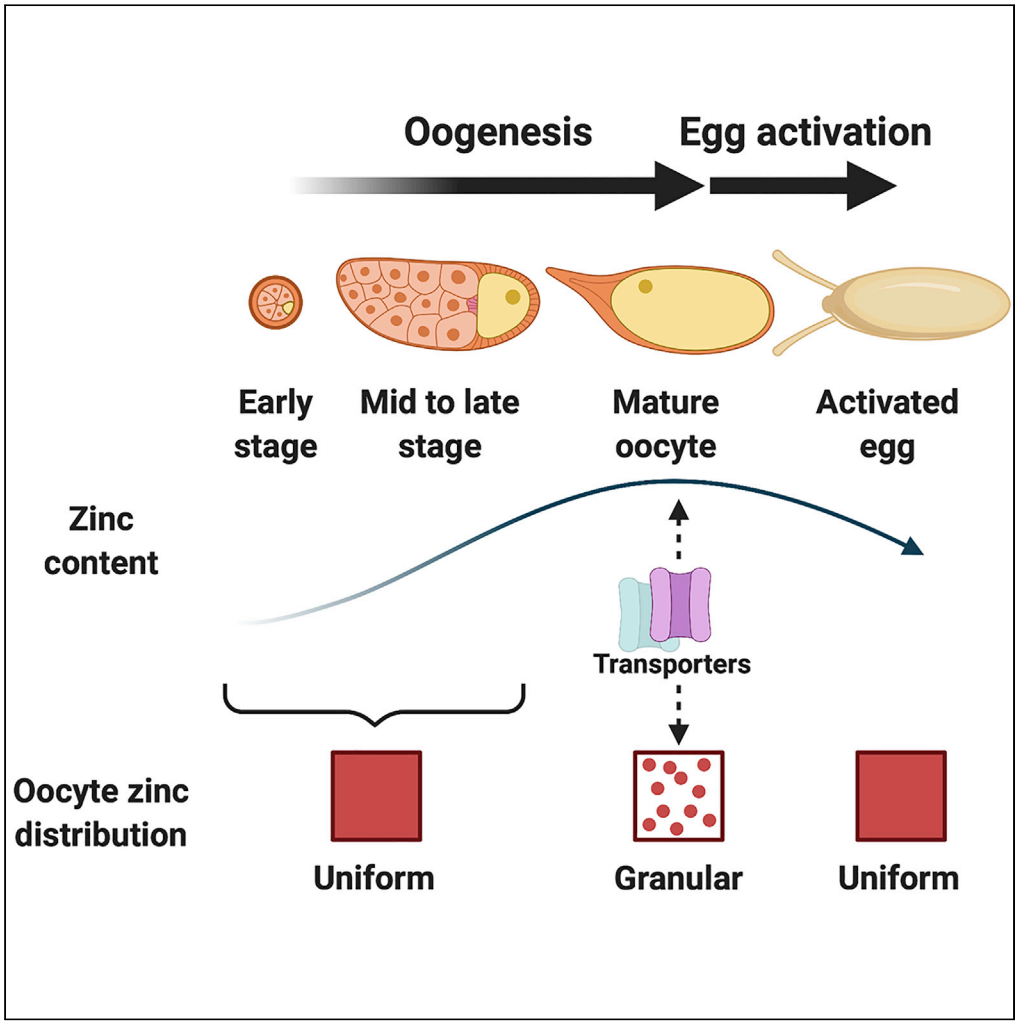

Qinan Hu, Francesca E. Duncan, Andrew B. Nowakowski, Olga A. Antipova, Teresa K. Woodruff, Thomas V. O'Halloran, Mariana F. Wolfner

tkw@northwestern.edu (T.K.W.)
t-ohalloran@northwestern.edu (T.V.O.)
mariana.wolfner@cornell.edu (M.F.W.)

HIGHLIGHTS

Dietary zinc is required for *Drosophila* female fertility

Oocyte zinc levels increase over oogenesis and decrease during egg activation

Zinc is enriched in the oocyte and forms aggregated granules in mature oocytes

Transporters are required for zinc retention and zinc-enriched granules in oocytes

Hu et al., iScience *23*, 101275
July 24, 2020
https://doi.org/10.1016/j.isci.2020.101275

iScience

CellPress
OPEN ACCESS

Article

Zinc Dynamics during *Drosophila* Oocyte Maturation and Egg Activation

Qinan Hu,[1] Francesca E. Duncan,[2] Andrew B. Nowakowski,[4,5] Olga A. Antipova,[3] Teresa K. Woodruff,[2,4,6,*] Thomas V. O'Halloran,[4,5,6,*] and Mariana F. Wolfner[1,7,*]

SUMMARY

Temporal fluctuations in zinc concentration are essential signals, including during oogenesis and early embryogenesis. In mammals, zinc accumulation and release are required for oocyte maturation and egg activation, respectively. Here, we demonstrate that zinc flux occurs in *Drosophila* oocytes and activated eggs, and that zinc is required for female fertility. Our synchrotron-based X-ray fluorescence microscopy reveals zinc as the most abundant transition metal in *Drosophila* oocytes. Its levels increase during oocyte maturation, accompanied by the appearance of zinc-enriched intracellular granules in the oocyte, which depend on transporters. Subsequently, in egg activation, which mediates the transition from oocyte to embryo, oocyte zinc levels decrease significantly, as does the number of zinc-enriched granules. This pattern of zinc dynamics in *Drosophila* oocytes follows a similar trajectory to that in mammals, extending the parallels in female gamete processes between *Drosophila* and mammals and establishing *Drosophila* as a model for dissecting reproductive roles of zinc.

INTRODUCTION

Transition metals such as iron, copper, and zinc ions bound tightly within enzymatic sites play a variety of well-established structural and catalytic roles within cells (Calap-Quintana et al., 2017; Egli et al., 2003). Among them, zinc is an important inorganic regulator of processes including cell proliferation, carbohydrate metabolism, and immunity (reviewed in Frassinetti et al., 2006; Roohani et al., 2013). Zinc can persist in cells as hydrated ions, bound to small metabolites as weakly bound complex ions or bound tightly in the active sites of zinc-dependent enzymes. Recent studies indicate that fluctuations in the availability of Zn^{2+} ions occur either through ionic fluxes (Bernhardt et al., 2012) or through covalent binding to metalloregulatory proteins (Gilston et al., 2014). Thus, this element serves alongside calcium and phosphorus as an inorganic signal mediator that can activate biological switching processes. One example of zinc as an inorganic signal occurs during mammalian oocyte maturation and embryogenesis. Specifically, zinc accumulates in maturing mouse oocytes from the arrest at prophase of meiosis I to the arrest at metaphase of meiosis II (MII) (Kim et al., 2010), and this increase is dependent on maternally derived zinc transporters ZIP6 and ZIP10 (Kong et al., 2014). When mature mouse oocytes are fertilized, thus "activating" them to complete meiosis and begin embryogenesis, there is a rapid release of zinc from the oocyte (Kim et al., 2011). Such "zinc sparks" have been observed in eggs upon activation in the mouse (Kim et al., 2011; Que et al., 2015; Zhang et al., 2016), cow (Que et al., 2019), and human (Duncan et al., 2016). This zinc release is dependent on calcium oscillations during egg activation (Kim et al., 2011; Suzuki et al., 2010) and is mediated by dynamic movement and exocytosis of zinc-loaded vesicles (Que et al., 2015; Tokuhiro and Dean, 2018). The programmed loss of cellular zinc through zinc sparks is associated with resumption of the cell cycle (Kim et al., 2011) and modification of the zona pellucida to block polyspermy (Que et al., 2017; Tokuhiro and Dean, 2018). After fertilization, regulation of zinc is required for the first mitotic divisions during embryogenesis (Kong et al., 2015). In another model organism, *C. elegans*, zinc is also required for oogenesis, meiotic progression (Hester et al., 2017), and embryo viability (Mendoza et al., 2017).

Drosophila's speed of development and excellent genetics makes it a tractable model to probe mechanisms and macromolecules of relevance to more complex systems, and its biology includes many parallels to events that occur in *Xenopus* and mammals, including in reproduction (Avila et al., 2010; Barnard et al., 2004; Bernhardt et al., 2018; Cui et al., 2008; Horner et al., 2006; Hu and Wolfner, 2019; Knapp and Sun, 2017; Mochida and Hunt, 2007; Pepling and Spradling, 2001; Takeo et al., 2006, 2010; Zhang et al.,

[1]Department of Molecular Biology and Genetics, Cornell University, Ithaca, NY 14853, USA

[2]Department of Obstetrics and Gynecology, Feinberg School of Medicine, Northwestern University, Chicago, IL 60611, USA

[3]X-ray Sciences Division, Argonne National Laboratory, Argonne, IL 60439, USA

[4]The Chemistry of Life Processes Institute, Northwestern University, Evanston, IL 60208, USA

[5]Department of Chemistry, Northwestern University, Evanston, IL 60208, USA

[6]Department of Molecular Biosciences, Northwestern University, Evanston, IL 60208, USA

[7]Lead Contact

*Correspondence: tkw@northwestern.edu (T.K.W.), t-ohalloran@northwestern.edu (T.V.O.), mariana.wolfner@cornell.edu (M.F.W.)

https://doi.org/10.1016/j.isci.2020.101275

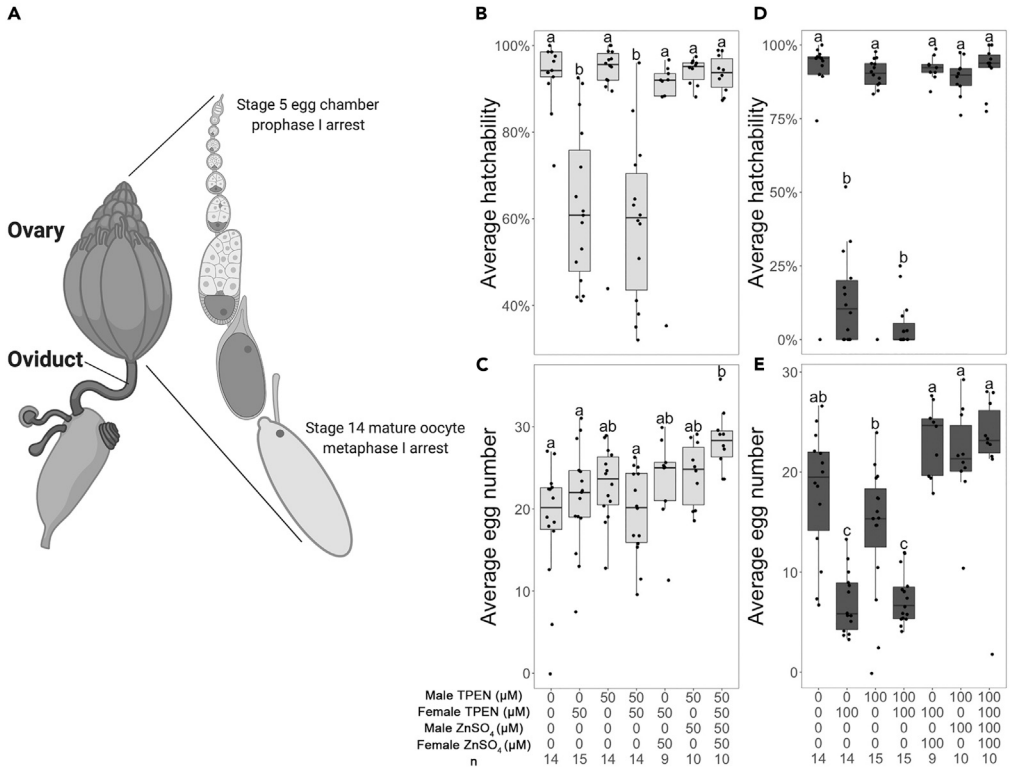

Figure 1. Dietary TPEN Impairs Female *Drosophila* Fertility

(A) Diagram of female *Drosophila* reproductive system, showing one of the pair of ovaries with enlarged view of the progressive stages in an ovariole. Meiotic stages during oogenesis are noted. Illustration created with Biorender.com. (B–E) Three-day average egg hatchability (B and D) and egg number (C and E) from single-pair crosses of ORP2 females and males with either or both sexes raised in 50 μM (B and C) or 100 μM (D and E) TPEN only or TPEN + $ZnSO_4$ rescue food. Male TPEN, concentration of dietary TPEN on which the males were raised and tested; female TPEN, concentration of TPEN added to food on which the females were raised and tested; male $ZnSO_4$, concentration of $ZnSO_4$ added to food on which the males were raised; female $ZnSO_4$, concentration of $ZnSO_4$ added to food on which the females were raised; n, sample size of each group; a, b, and c, significance groups (significant difference of mean with $p < 0.05$ between groups with different labels). Whiskers on the boxplots show the top and bottom quartiles.

2018). As in other animals, *Drosophila* oocytes develop through a stepwise process of stages, 14 in this case, making it straightforward to examine zinc dynamics during oogenesis. Specifically, a cystoblast, the destined-to-differentiate daughter of a female germline stem cell, undergoes four mitotic divisions with incomplete cytokinesis to result in a 16-cell cyst. One of the 16 cells becomes the oocyte; her 15 sisters, the nurse cells, synthesize macromolecules, organelles, and other components that will be transferred into the oocyte as oogenesis progresses. Meiosis starts at early stage of oogenesis and arrests at prophase I at stage 5. This arrest lasts until stage 13 when meiosis progresses to metaphase I (MI) (von Stetina and Orr-Weaver, 2011). At later stages of oogenesis, nurse cells undergo apoptosis. The mature (stage 14) oocyte remains meiotically arrested at MI until ovulation (Figure 1A) (reviewed in Avilés-Pagán and Orr-Weaver, 2018; Bastock and St Johnston, 2008; McLaughlin and Bratu, 2015). Then, mechanical forces due to passage into the oviduct and/or swelling of the oocyte as it takes up oviductal fluid "activate" the egg (Heifetz et al., 2001, reviewed in Carlson, 2019; Horner and Wolfner, 2008a). As in mammals, egg activation in *Drosophila* involves a rise in internal free calcium levels (Kaneuchi et al., 2015; York-Andersen et al., 2015), progression through meiosis, and changes in the egg's transcriptome, proteome, and envelopes (reviewed in Horner and Wolfner, 2008a; Kashir et al., 2014; Krauchunas et al., 2013; Sartain and Wolfner, 2013; Swann and Lai, 2016). The process of egg activation can be largely, although not perfectly, mimicked *in vitro* by submerging isolated mature oocytes in a hypotonic buffer (Horner and Wolfner, 2008b; Page and Orr-Weaver, 1997).

Given the importance of zinc dynamics during mammalian and *C. elegans* oocyte maturation and egg activation, we asked if similar processes occur in *Drosophila* as well. Interestingly, in a previous proteomic study that looked at phospho-modulation of maternal proteins during the transition from egg to embryo, we noticed that Znt35C, the most highly expressed zinc transporter in the *Drosophila* ovary (Leader et al., 2017), undergoes phospho-state change during egg activation, suggesting that its activity might be modulated during egg activation (Zhang et al., 2018). Znt35C is one of the transporters that regulates the biogenesis of lysosome-related zinc storage granules in *Drosophila* malpighian tubules (Tejeda-Guzmán et al., 2018), excretory organs that are a site of very active zinc homeostasis regulation.

To further examine the role of zinc in *Drosophila* reproduction, we first tested whether zinc is important for fertility. We observed that females fed a zinc-deficient diet had impaired fertility. This prompted us to examine the dynamics of zinc in their germline. Using synchrotron-based X-ray fluorescence microscopy (XFM), we tracked the distribution and dynamics of zinc and other transition metals throughout *Drosophila* oogenesis and egg activation. We observed that zinc is the most abundant transition metal in *Drosophila* oocytes and eggs. Total intracellular zinc levels increase during oogenesis, accompanied by formation of zinc-enriched granules in the oocyte cytoplasm. The maintenance of these zinc granules in mature oocytes depends on transporters. Upon egg activation, there is a significant decrease in intracellular zinc levels and in the presence of zinc granules in wild-type oocytes. All these observations are reminiscent of zinc dynamics seen in mammalian oocyte maturation and egg activation.

RESULTS

Dietary Zinc Deficiency Reduces Female *Drosophila* Fertility

Given the importance of zinc in the mammalian and *C. elegans* oocyte, we began by testing whether zinc is essential for female fertility in *Drosophila*. We followed protocols analogous to those reported for *C. elegans* (Hester et al., 2017), where addition of the zinc chelator, N,N,N′,N′-tetrakis(2-pyridylmethyl)-1,2-ethylenediamine (TPEN) to the food at a concentration of 50 μM significantly impairs *C. elegans* fertility. We raised Oregon-R-P2 (ORP2; wild-type) (Allis et al., 1977) flies on food containing 50 or 100 μM TPEN and assessed their fecundity and egg hatchability (percent of eggs that are able to hatch) on food containing TPEN. We tested single-pair crosses, in which one or both partners had been raised on food containing TPEN and compared them with control crosses, in which both partners had been raised on control food. Males raised on 50 or 100 μM TPEN food were not impaired in siring offspring; their mates laid normal numbers of eggs that had normal hatchability (Figures 1B–1E). Female flies raised on either 50 or 100 μM TPEN-treated food exhibited reduced egg hatchability; the effect was more severe at a higher dosage of TPEN, regardless of whether their mates came from control or TPEN food (Figures 1B and 1D). It was observed that 50 μM TPEN-treated females displayed reduced egg hatchability only beginning on day 2 postmating (Figure S1A). To test if this was the result of residual zinc from their parents, who had been reared on untreated food and transferred to TPEN-treated food after eclosion, we repeated the assay using female offspring of TPEN-treated flies that themselves had been reared on TPEN-treated food. We observed the same trend (Figure S1B), suggesting that addition of 50 μM TPEN to food leads to a delayed reduction in egg hatchability. Females raised on 50 μM TPEN laid normal numbers of eggs (Figure 1C), whereas females raised on 100 μM TPEN produced significantly fewer eggs (Figure 1E). All these adverse effects on female fertility were rescued by supplementation with $ZnSO_4$ at equimolar concentrations to the TPEN in the food (Figures 1B–1E), confirming the requirement of zinc for female fertility. Thus, dietary zinc is required for female *Drosophila* fertility, but does not appear to affect male fertility. Moreover, zinc insufficiency impacts both the quality and quantity of oocytes.

As TPEN also has a high affinity for copper (Percival and Layden-Patrice, 1992), we attempted to test the effects of two copper chelators, neocuproine and ammonium tetrathiomolybdate (TM), on *Drosophila* female fertility. Unfortunately, at all concentrations tested (25, 50, and 100 μM, based on comparative concentrations of TPEN), presence of either chelator in the medium was either toxic or semitoxic to the flies (neocuprione) or slowed the flies' development by > 3-fold (TM), indicating a negative effect on fitness. Thus, although the surviving females had lower egg-laying ability and hatchability than normal (reduction of 13%, 73% for 25 μM neocuprione; 41%, 88% for 50 μM neocuprione; 63%, 91% for 25 μM TM; and 52%, 95% for 50 μM TM, respectively), this cannot be considered direct effects of either chelator on the female

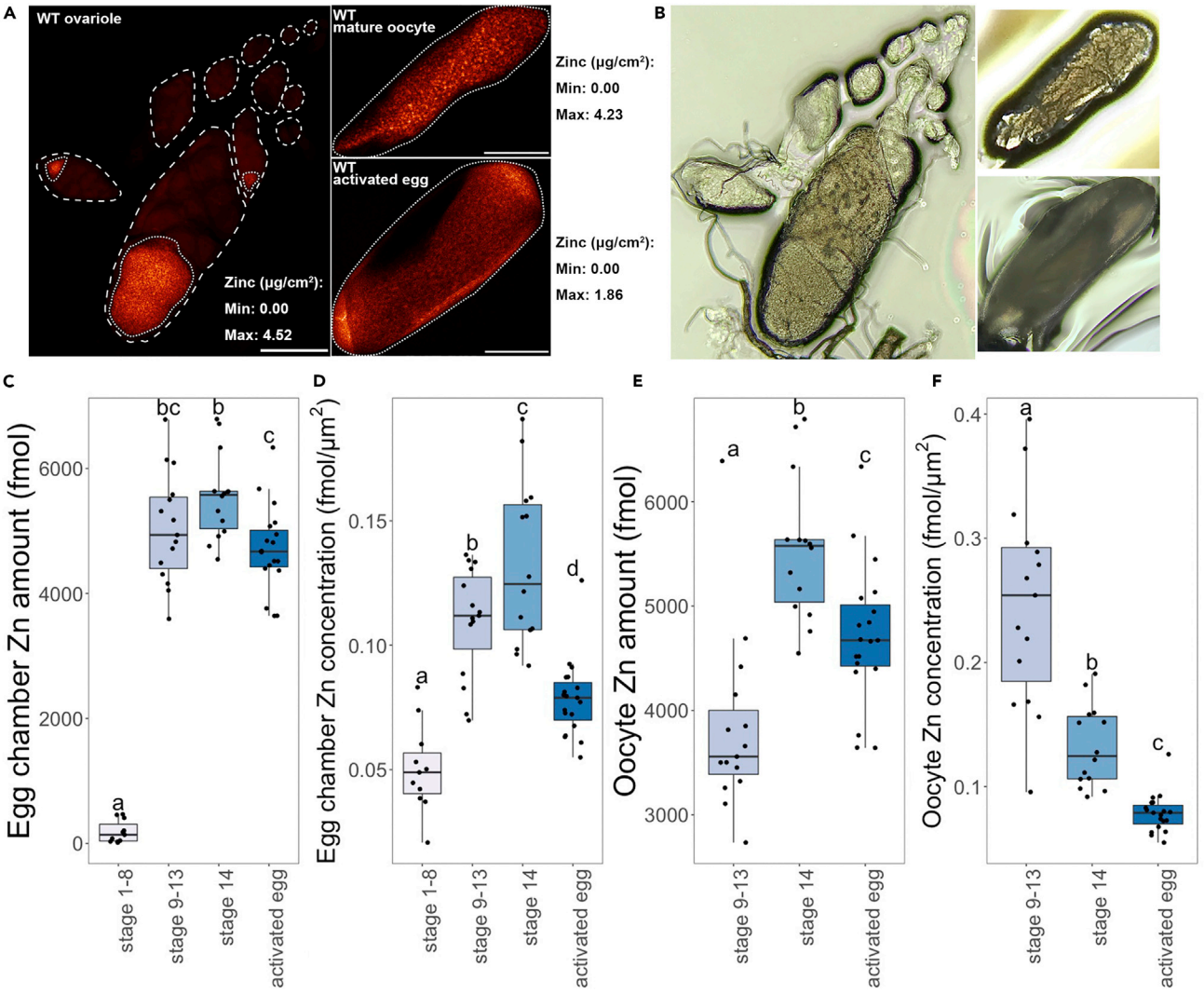

Figure 2. Zinc Level and Distribution Changes during Oocyte Maturation and Egg Activation in Wild-Type *Drosophila*

(A) Representative XFM images showing zinc distribution in egg chambers at different stages of oogenesis and egg activation. Left, an ovariole containing immature egg chambers up to stage 10; upper right, a stage 14 mature oocyte; lower right, an activated but unfertilized egg. Dashed lines delineate the outline of egg chambers. Dotted lines delineate the outline of oocytes in stage 9–13 egg chambers, mature oocytes, and activated eggs.

(B) Bright-field image of samples scanned in (A). Due to dehydration during sample preparation, morphology of these egg chambers does not completely reflect their *in vivo* state. All scale bars, 100 µM.

(C–F) Total zinc content (C and E) and zinc concentration (D and F) of zinc in egg chambers (C and D) and oocytes (E and F). Stage 1–8 oocytes n = 11, stage 9–13 oocytes n = 15, stage 14 oocytes n = 14, activated eggs n = 19. a, b, c, and d, significance groups (significant difference of mean with $p < 0.05$ between groups with different labels). Whiskers on the boxplots show the top and bottom quartiles.

germline; it is likely a consequence of the toxicity/negative fitness effects of the chelator to the fly as a whole.

Zinc Is the Most Abundant Transition Metal Measured in *Drosophila* Oocytes and Activated Eggs

Given the importance of zinc in mammalian and *C. elegans* gamete biology and the effect of dietary zinc deficiency in female *Drosophila* fertility, we measured and visualized the subcellular distribution of total zinc as well as other transition elements in oocytes from ORP2 females using synchrotron-based XFM. We examined four groups of egg chambers and eggs throughout development: early-stage oogenesis (stages 1–8), mid/late-stage oogenesis (stages 9–13), mature oocytes (stage 14), and activated (laid,

unfertilized) eggs (Figures 2A and 2B). XFM data provide the content measurements of a sample through detection of element-specific X-ray emission spectra. The total amount of each element (in fmol) was calculated from data integrated along the z axis of the scans of each sample. Element distributions were represented as two-dimensional projection images with total element content measurements. We analyzed the element contents of the egg chambers (including nurse cells and oocytes) as well as the oocytes alone (for stages with clearly observable oocytes). The oocyte can be distinguished as the most posterior cell within the egg chamber. As nurse cells dump their cytoplasm into the oocyte during late oogenesis (reviewed in Cavaliere et al., 1998), the element contents of mature oocytes and activated eggs should include those from both nurse cells and oocytes from earlier stages of oogenesis. We also attempted to quantify element concentration in scanned samples. As the volumes of egg chambers were difficult to measure due to their irregular shape, we used total element amounts in the region of interest (ROI) divided by the area of ROI as an approximate of element concentration.

Consistent with their important physiological roles, zinc, iron, and copper were the most abundant transition metals measured across all stages of oogenesis and after egg activation. Among these three, zinc was present in the highest molar amount with 5,543 $\pm$ 684 fmol in mature oocytes, compared with 2,188 $\pm$ 344 fmol of iron and 198 $\pm$ 49 fmol of copper in mature oocytes (mean $\pm$ SEM, Figure S2A). This is analogous to the relative amounts of transition metals in mammalian oocytes and embryos (Kim et al., 2010).

Fluxes in Total Zinc Occur during Oocyte Maturation and Egg Activation

XFM showed increases in iron, copper, and zinc content as egg chambers transitioned from early to mid/late oogenesis. Before about stage 9, there are on average 6.24 $\pm$ 5.71 fmol of copper, 112 $\pm$ 95 fmol of iron, and 186 $\pm$ 178 fmol of zinc in each egg chamber. After stage 9, each egg chamber contained on average 156 $\pm$ 36 fmol of copper, 2,174 $\pm$ 307 fmol of iron, and 5,045 $\pm$ 879 fmol of zinc (mean $\pm$ SEM, Figure S2A). Interestingly, as the amount of these transition metals increased within egg chambers in mid-late oogenesis, copper, iron, and zinc became more concentrated in the oocyte, relative to the associated nurse cells. In stage 9–13 egg chambers, 71.1% copper, 51.5% iron, and 75.9% zinc were enriched in the oocyte, on average (Figures 2A and S3B).

From mid/late oogenesis stages to stage 14 and egg activation *in vivo*, both the amount and area concentration of iron and copper remained constant with no statistical differences in either egg chambers or oocytes alone (Figure S2). However, both the zinc content (fmol) and the zinc concentration (fmol/μm^2) underwent dynamic changes (Figures 2C–2F and S2). When considering the entire egg chamber, zinc concentration significantly increased from stage 9–13 to stage 14 (Figure 2D). Zinc content and concentration significantly dropped from stage 14 oocytes to eggs activated *in vivo* (Figures 2C and 2D). When looking at the oocyte alone, zinc amount significantly increased from stage 9–13 to stage 14 and also significantly decreased from stage 14 to activated eggs (Figure 2E). Interestingly, oocyte zinc concentration kept dropping significantly as the oocytes progressed from stage 9–13 to stage 14 and from stage 14 to activated eggs *in vivo* (Figure 2F).

To rule out the possibility that the zinc level changes we observed were due to fluctuations of metal levels in general, we reanalyzed our data by normalizing the amount of zinc to that of iron. We saw the same trend: egg chamber zinc concentration rose significantly during oogenesis and dropped significantly during egg activation, and oocyte zinc concentration dropped significantly from stage 9–13 to stage 14 and from stage 14 to activated eggs (Figure S4).

Taken together, these data indicate that zinc content keeps increasing in the egg chamber over oogenesis but decreases after egg activation. Within the egg chamber, zinc becomes more and more enriched in the oocyte in the egg chamber over oogenesis before a significant decrease during egg activation. The reduced concentration from stage 9–13 to stage 14 mature oocyte (Figure 2F) is possibly due to nurse cell dumping, in which the zinc-enriched oocyte cytoplasm is mixed with the nurse cell cytoplasm containing less zinc.

Zinc-Enriched Granules Form during Oocyte Maturation and Diminish during Egg Activation

Although copper and iron displayed generally uniform distributions within the oocyte (Figures 3A and 3B), the zinc distribution became punctate over development (Figures 3A, 3A′, S3A, and S3B). In stage 14 mature oocytes, zinc was seen in distinct granules (Figures 3B, 3B′, S3C, and S3D). However, during egg

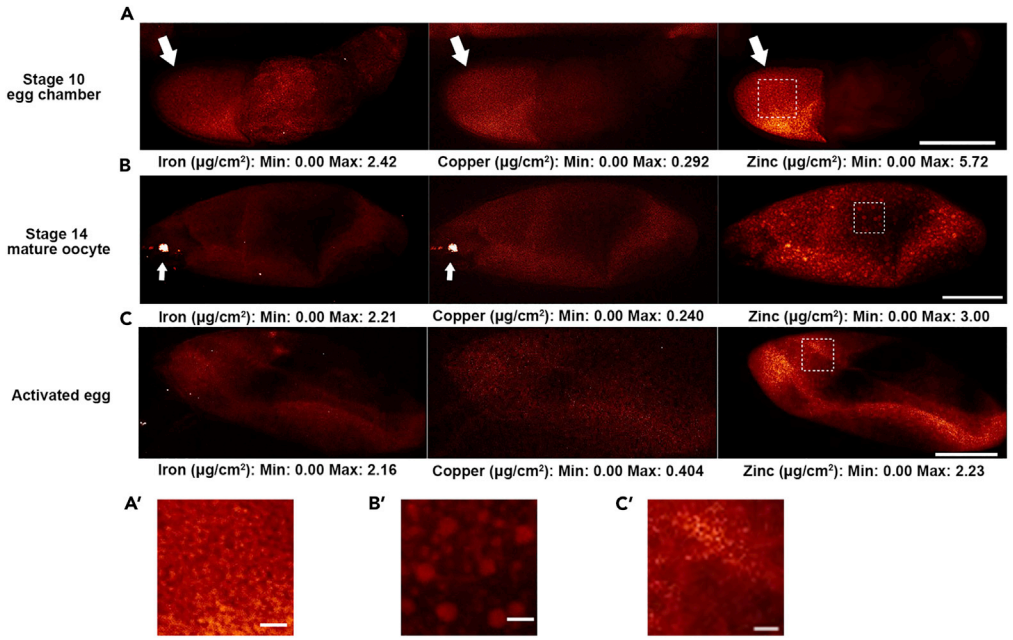

Figure 3. Distribution of Iron, Copper, and Zinc during Oocyte Maturation and Egg Activation in Wild-Type *Drosophila*

(A–C) Representative XFM images showing iron, copper, and zinc distribution in (A) an egg chamber around stage 10. Within an egg chamber, iron, copper, and zinc are all more concentrated in the oocyte (arrows); (B) a mature oocyte (stage 14). Zinc displays a more granulated distribution compared with iron and copper. Iron and copper display an even distribution. A granule of highly concentrated iron and copper (arrows) was observed at the anterior end of 8 of 14 of the wild-type mature oocytes, at approximately the location of the future micropyle, and egg anterior cytoplasm (see additional examples in Figure S9). The nature of this granule is unknown; (C) an activated but unfertilized egg. Zinc displays an even distribution. All samples are from ORP2 wild-type females. Scale bars, 100 μm. (A′–C′) Enlarged view of zinc distribution in (A–C). Dashed squares indicate enlarged regions. Scale bars, 10 μm.

activation, as intracellular zinc levels decreased, these zinc granules also decreased in number (Figures 3C, 3C′, S3E, and S3F). These data suggest that these granules may store zinc during oocyte maturation before the loss observed following egg activation. To further test for the existence of a granular or organellar basis for the distribution of zinc, we used a centrifugation protocol. Such treatment of *Drosophila* embryos is known to stratify their subcellular components (Tran and Welte, 2010). In activated eggs whose cytoplasm was stratified in this manner, the majority of iron, copper, and zinc became localized at the posterior end of the centrifuged eggs (Figure S5). This is where heavier organelles pellet, consistent with zinc being in or associated with organellar granules in the eggs. We could not examine the results for mature oocytes because they all collapsed during centrifugation, likely due to their fragile eggshells (Heifetz et al., 2001, reviewed in Horner and Wolfner, 2008a).

Transporters White (W) and Znt35C are important in the biogenesis of zinc storage granules in *Drosophila* malpighian tubules, an excretory tissue that is the *Drosophila* counterpart of the mammalian kidney (Tejeda-Guzmán et al., 2018). In particular, Znt35C (the ortholog of mammalian ZNT2/ZNT3/ZNT8), which localizes to the membranes of zinc storage granules in malpighian tubules (Tejeda-Guzmán et al., 2018), is the most highly expressed zinc transporter in the *Drosophila* ovary (Leader et al., 2017) and is regulated by phosphorylation during egg activation (Zhang et al., 2018). We generated a *znt35C*^{1} null mutation using CRISPR/Cas9; for technical reasons (Figure S10) our mutant strain also carried a mutation in the *w* gene. A previously published, but unavailable, *znt35C* null mutant had been reported to be viable unless exposed to excessive zinc (Yepiskoposyan et al., 2006); our *znt35C*^{1} mutant was similarly viable on normal food. Thus, we were able to isolate oocytes at all developmental stages from homozygous *znt35C*^{1} females and subject them to XFM analysis (Tejeda-Guzmán et al., 2018).

Our XFM data showed that zinc is present during oogenesis in *w; znt35C*^{1} mutants and was still the transition metal with the highest amount and concentration in egg chambers and oocytes (Figures S6A–S6D). As

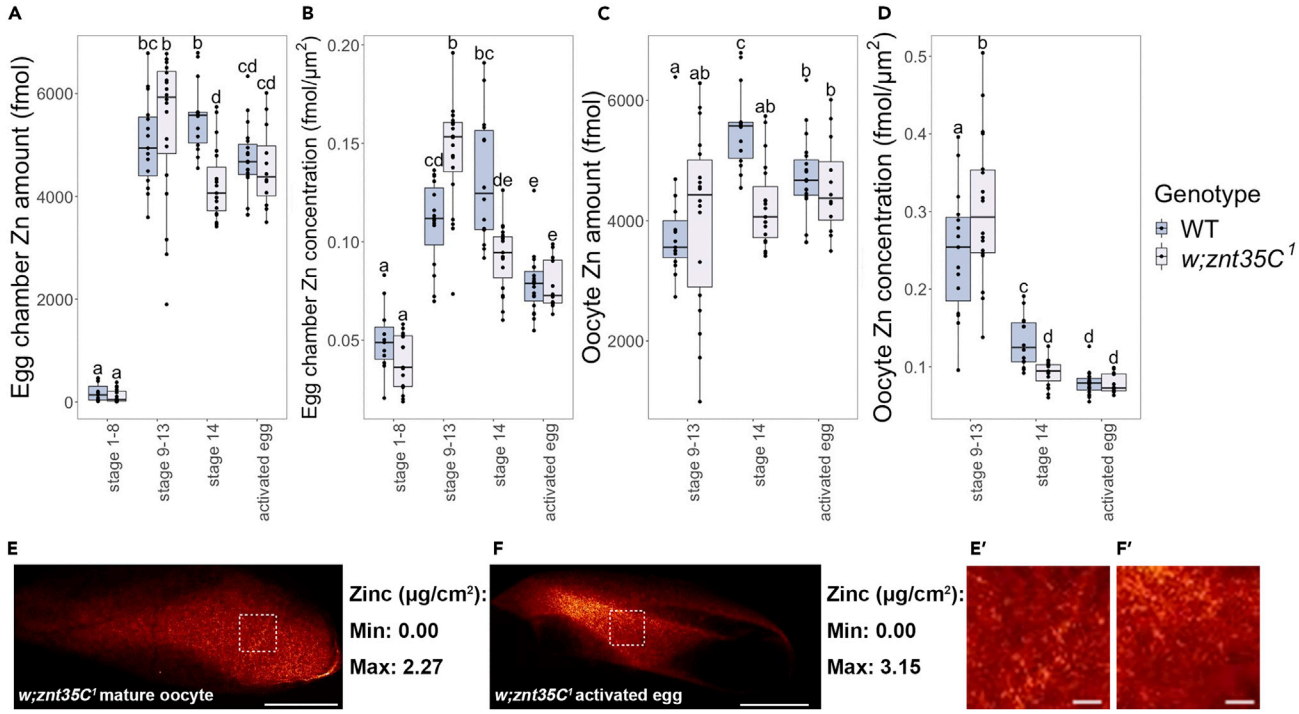

Figure 4. Zinc Distribution and Quantification Over Oocyte Maturation and Egg Activation in *w; znt35C¹* *Drosophila*

(A–D) The total zinc content (A and C) and zinc concentration (B and D) in each egg chamber (A and B) and oocyte (C and D) of *w; znt35C¹* compared with ORP2 wild-type. WT: ORP2 wild-type. KO: *w; znt35C¹* null mutant. Stage 1–8 oocytes: WT n = 11, KO n = 15; stage 9–13 oocytes: WT n = 15, KO n = 20; stage 14 oocytes: WT n = 14, KO n = 19; activated eggs: WT n = 19, KO n = 12. a, b, c, d, and e: significance groups (significant difference of mean with $p < 0.05$ between groups with different labels). Whiskers on the boxplots show the top and bottom quartiles. (E and F) Representative XFM images showing zinc distribution in (E) a mature oocyte at stage 14 and (F) an activated but unfertilized egg from *w; znt35C¹* mutant females. Scale bars, 100 μm. (E′ and F′) Enlarged view of (E and F). Dashed squares indicate enlarged regions. Scale bars, 10 μm.

in the wild-type animals, iron, copper, and zinc were enriched in the oocyte relative to the whole egg chamber in the mutants (Figures S6E and S6E′). *w; znt35C¹* egg chambers displayed accumulation of zinc from stage 1–8 to stage 9–13 of oogenesis similar to wild-type (Figures 4A and 4B). However, *w; znt35C¹* oocytes contained more zinc than wild-type oocytes in stage 9–13 when looking at the egg chamber or the oocyte alone. This difference was statistically significant with regard to zinc concentration in egg chambers (Figure 4B) and oocytes (Figure 4D). In contrast, wild-type stage 14 mature oocytes displayed significantly higher zinc content and concentration than stage 14 oocytes of *w; znt35C¹* (Figures 4A and 4B). When looking at the oocyte alone, unlike that in wild-type oocytes, zinc amounts in *w; znt35C¹* oocytes remained constant from stage 9–13 to stage 14 and from stage 14 to activated eggs (Figure 4C). These trends remained the same when zinc content was normalized to iron content (Figure S4). Zinc granules were also largely absent from *w; znt35C¹* mature oocytes (Figures 4E, 4E′, S6F, and S6F′) or activated eggs (Figures 4F, 4F′, S6G, and S6G′). However, *w; znt35C¹* females did not display defects in egg production or hatchability (Figure S7), suggesting that the accumulation of zinc in mature oocytes is not solely (or non-redundantly) necessary for *Drosophila* fertility under zinc-sufficient conditions.

Taken together, our data showed that in *w; znt35C¹* mutants, zinc accumulates more in egg chambers and enriches more in oocytes compared with wild-type before stage 14. At stage 14, *w; znt35C¹* oocytes fail to retain zinc as well as wild-type does, concurrent with the absence of zinc-enriched granules. A subsequent zinc decrease during egg activation, observed in wild-type, is not observed in *w; znt35C¹* mutants. Our data suggest that one or both of these transporters have roles in transporting zinc out of egg chambers before oocyte maturation and/or roles in retaining zinc in mature oocytes by maintaining zinc-enriched granules; future studies will tease apart the roles of these two transporters in zinc homeostasis.

DISCUSSION

Zinc is essential for life and necessary for reproductive functions and fertility in *C. elegans* and several mammalian species. However, the requirement for zinc in fertility and its levels and distributions in oocytes and after oogenesis were unknown for any arthropod, including the major model system, *Drosophila*. Here, we determined that dietary zinc is essential for *Drosophila* female fertility. This prompted us to use XFM to examine zinc distribution during oogenesis and egg activation. We found that zinc is the most abundant transition metal in *Drosophila* oocytes at all stages. Zinc levels increase during oogenesis, and within the egg chamber, zinc becomes concentrated in the oocyte. Mature oocytes have high levels of zinc in aggregates or granules. Egg activation coincides with loss of both zinc and granules from the oocyte. As discussed later in the article, the loading of zinc into oocyte granules and the loss of zinc upon egg activation are conserved between fly and mammalian oocyte biology.

Zinc Is Required for Female Fertility in *Drosophila*

Dietary zinc is necessary for female fertility in *Drosophila*, impacting both the quality and quantity of eggs produced, suggesting the fly as a possible model for studying zinc-related subfertility. In mammalian females, zinc also plays multiple roles in oocytes across various stages. Dietary zinc depletion leads to premature germinal vesicle breakdown, spindle defects during oocyte maturation, and blocked ovulation and epigenetic programming alterations (Tian and Diaz, 2013, 2012). After fertilization, zinc deficiency further perturbs chromatin structure, reduces global transcription, and disrupts placental development during early embryogenesis (Kong et al., 2015; Tian et al., 2014). In *C. elegans* hermaphrodites, dietary zinc deficiency results in impaired oogenesis and chromosome dynamics during meiosis in the germline, which reduces brood size and embryo viability (Hester et al., 2017; Mendoza et al., 2017). Interestingly, we did not see impairment of male fertility upon zinc depletion in *Drosophila* males, even though in mammals zinc deficiency is associated with sperm chromatin instability and thus male infertility (Caldamone et al., 1979; Kvist et al., 1987). This observation is analogous to *C. elegans*, in which oocytes are more sensitive to zinc deprivation than sperm (Mendoza et al., 2017). It is still possible that the levels of TPEN we tested in *Drosophila*, although sufficient to impair female fertility, were too low to affect spermatogenesis. In addition, dietary zinc deficiency could also lead to impaired female fertility in a systematic and indirect way instead of through a direct impact on oogenesis. These possibilities are subjects for future studies.

Transporters Are Required for the Maintenance of Zinc Storage Granules in *Drosophila* Oocytes

During *Drosophila* oocyte maturation, the presence of zinc-enriched granules is maintained by zinc transporter Znt35C and/or the ABC transporter W; future studies are required to distinguish their relative contributions. *Drosophila* Znt35C and W are also involved in the biogenesis of lysosome-related zinc granules, which function as the major zinc reservoir in principal malpighian tubule epithelial cells (Tejeda-Guzmán et al., 2018). It is thus tempting to speculate that similar mechanisms are used in the *Drosophila* oocyte to store its high levels of zinc during maturation in preparation for zinc release upon egg activation. Consistent with this interpretation, we observed that *w; znt35C*^{1} null mutant females fail to maintain high levels of zinc or zinc granules in their mature oocytes and consequently show no decrease in zinc levels upon egg activation.

In mammalian egg activation, zinc is released from zinc-loaded vesicles undergoing exocytosis after fertilization (Que et al., 2015). Given that zinc granules in wild-type *Drosophila* mature oocytes are largely absent after egg activation, they may serve similar purposes in packaging zinc for traffic out of oocytes during egg activation. It will be intriguing in this context to examine the role of the mammalian orthologs of W (ABCG2) and of Znt35C (ZNT2/ZNT3/ZNT8; members of the SLC30 [ZnT] family of membrane proteins, which transport zinc out of the cytosol, some of which are localized in the plasma membrane and others in intracellular compartments; reviewed in Schweigel-Röntgen, 2014) in organizing and maintaining zinc levels in mammalian oocytes and in the mechanics of zinc release upon fertilization.

Zinc Dynamics during Oocyte Maturation and Egg Activation in *Drosophila* and Mammals

In multiple mammalian species, zinc levels are high in oocytes but drop dramatically during egg activation via a series of exocytotic events termed zinc sparks (Duncan et al., 2016; Kim et al., 2011; Que et al., 2019; Zhang et al., 2016). In mice, the zinc spark occurs coordinately with and is dependent on calcium oscillations during egg activation (Kim et al., 2011) and plays multiple roles in downstream events of egg activation including resumption of cell cycle (Kim et al., 2011) and modification of the zona pellucida (Que et al.,

2017). Our observation of a decrease in zinc levels in *Drosophila* oocytes during egg activation parallels what is seen in mammals at this time, suggesting an overall analogy in phenomena, and the potential for *Drosophila* to serve as a model for dissecting zinc flux mechanisms. In mouse, mature oocytes arrest at MII stage of meiosis when intracellular zinc level peaks. The zinc spark is required for release of MII arrest and completion of meiosis (Kim et al., 2011). *Drosophila* mature oocytes arrest at MI of meiosis. Meiosis also completes after egg activation. It is possible that more complex zinc fluxes occur as meiosis progresses during egg activation (e.g., increase before MII and decrease afterward, parallel to that in mouse). However, as we only examined oocyte samples before and after egg activation here, the presence of such dynamics is a subject of future studies.

Interestingly, we did not see a decrease in zinc granules following *in vitro* activation (Figures S8A and S8A'); similarly, we only saw the decrease in zinc levels during egg activation *in vivo* but not after *in vitro* egg activation (Figure S8B). There are two possible explanations for this difference between eggs activated *in vivo* and *in vitro*. It is possible that zinc release and reduction of zinc granules occurs after the 30-min window used for the *in vitro* experiments. Alternatively, *in vitro* activation is known not to be completely physiological (Horner and Wolfner, 2008b; Page and Orr-Weaver, 1997), and it may thus fail to modulate zinc levels appropriately. However, the failure of zinc changes *in vitro* to match those seen *in vivo* made it impossible for us to directly observe zinc release real-time in *Drosophila* egg activation with fluorescent zinc markers.

Our findings that zinc accumulates during *Drosophila* oogenesis, becomes concentrated in granules in the mature oocyte, and eventually decreases after egg activation suggests possible conservation of zinc dynamics from *Drosophila* to those in *C. elegans* and mammals. Similar mechanisms (e.g., homologous zinc transporters) may be involved in zinc homeostasis regulation during oocyte maturation and egg activation. This strongly motivates the studies of these parallel processes from *Drosophila* to *C. elegans* and mammals.

Limitations of the Study

The irregular shape of the oocytes, particularly after the required dehydration, prevented precise calculation of the concentration of elements measured by dividing the total elemental content by the volume of egg chambers or oocytes. We divided the total elemental content by the area of ROI as an approximation. The relative data are correct, but the absolute number may have an incalculable slight margin of error. In the future, we may be able to approximate oocyte volumes by expressing fluorescent plasma membrane markers throughout oogenesis, acquiring z stack images of egg chambers with confocal imaging, reconstructing the 3D model of egg chambers, and measuring its volume. Using this approach, we could better assess an average egg chamber volume at different stages of oogenesis for more precision in element concentration.

As XFM only provides 2D images stacked along the z axis of scanned samples, we were unable to quantify the number and size changes of zinc-enriched granules or determine their intracellular localization through oogenesis and egg activation. Such experiments may reveal the molecular nature of these granules and will be the subject of future studies.

To investigate the role of Znt35C mutant, we generated a *znt35C*^{1} null mutant strain using CRISPR/Cas9. However, due to technical limitations, our mutant strain was in the *w*- background. Mutations in *w* impact the zinc physiology of flies, including their zinc storage ability (Afshar et al., 2013; Tejeda-Guzmán et al., 2018). Thus, we were unable to determine if the reduction in zinc levels and zinc granule numbers were results from mutation of *w*, *znt35C*, or both. Future analysis of samples from *w+*; *znt35C*^{1} will be required to clarify this.

Resource Availability

Lead Contact

M.F. Wolfner (mariana.wolfner@cornell.edu) is the lead contact for this paper.

Materials Availability

The *w*; *znt35C*^{1} mutant strain is available upon request from M. Wolfner.

Data and Code Availability

The XFM raw data are available at https://drive.google.com/drive/folders/1O9wDQbawoZ2Ytp9LwcLB2hCFDFwATuXe?usp=sharing; R codes used for analysis and plotting are available at https://github.com/WolfnerLab/zinc_reproduction.

METHODS

All methods can be found in the accompanying Transparent Methods supplemental file.

SUPPLEMENTAL INFORMATION

Supplemental Information can be found online at https://doi.org/10.1016/j.isci.2020.101275.

ACKNOWLEDGMENTS

This research used resources of the Advanced Photon Source, a US Department of Energy (DOE) Office of Science User Facility operated for the DOE Office of Science by Argonne National Laboratory under Contract No. DE-AC02-06CH11357. We thank Cornell's graduate school travel award (to Q.H.) and George P. Hess travel award (to Q.H.); National Institutes of Health grants R01-GM115848 (to T.K.W. and T.V.O.), R01-GM038784 (to T.V.O.), and R21-HD088744 (to M.F.W.); Postdoctoral Individual National Research Service Award F32-GM115052 (to A.B.N.); and Stephen H. Weiss Presidential Fellowship (to M.F.W.) and Barbara Payne Memorial Funds (to M.F.W.) for funding this study. We thank Dr. Robert A. Holmgren for rearing flies for some of the experiments. We thank Dr. Yasir Ahmed-Braimah for suggesting the egg centrifugation experiment and Drs. J. Liu, =C. Han, S. Garwin, and three anonymous reviewers for helpful comments on the manuscript. We thank Adriana N. Vélez-Avilés for assistance with *znt35C*^{1} mutant strain screening and Lauryn A. Worley for assistance with the TPEN fertility assays, and the Society for Developmental Biology's "Choose Development!" fellows' program (NSF grants IOS-1239422 and REU DBI-1156528) and Cornell Molecular Biology and Genetics department's Research Experience for Undergraduates (NSF grant REU DBI-1659534) program for supporting them. We thank Cornell's Statistical Consulting Unit for assistance with data analysis. The diagrams for the Graphical Abstract were created using Biorender.

AUTHOR CONTRIBUTIONS

Conceptualization, Q.H., F.E.D., and M.F.W; Investigation, Q.H., F.E.D., A.B.N., and O.A.A.; Data Analysis, Q.H., O.A.A., F.E.D., M.F.W., T.K.W., and T.V.O.; Writing, Q.H.; Editing, Q.H., F.E.D., A.B.N., O.A.A., T.K.W., T.V.O., and M.F.W.; Funding Acquisition, T.K.W., T.V.O., and M.F.W.

DECLARATION OF INTERESTS

The authors declare no conflict of interests.

Received: April 17, 2020
Revised: May 30, 2020
Accepted: June 11, 2020
Published: July 24, 2020

REFERENCES

Afshar, N., Argunhan, B., Bettedi, L., Szular, J., and Missirlis, F. (2013). A recessive X-linked mutation causes a threefold reduction of total body zinc accumulation in *Drosophila melanogaster* laboratory strains. FEBS Open Biol. *3*, 302–304.

Allis, C.D., Waring, G.L., and Mahowald, A.P. (1977). Mass isolation of pole cells from *Drosophila melanogaster*. Dev. Biol. *56*, 372–381.

Avila, F.W., Sirot, L.K., LaFlamme, B.A., Rubinstein, C.D., and Wolfner, M.F. (2010). Insect seminal fluid proteins: identification and function. Annu. Rev. Entomol. *56*, 21–40.

Avilés-Pagán, E.E., and Orr-Weaver, T.L. (2018). Activating embryonic development in *Drosophila*. Semin. Cell Dev. Biol. *84*, 100–110.

Barnard, D.C., Ryan, K., Manley, J.L., and Richter, J.D. (2004). Symplekin and xGLD-2 are required for CPEB-mediated cytoplasmic polyadenylation. Cell *119*, 641–651.

Bastock, R., and St Johnston, D. (2008). *Drosophila* oogenesis. Curr. Biol. *18*, R1082–R1087.

Bernhardt, M.L., Kong, B.Y., Kim, A.M., O'Halloran, T.V., and Woodruff, T.K. (2012). A zinc-dependent mechanism regulates meiotic progression in mammalian oocytes. Biol. Reprod. *86*, 111–114.

Bernhardt, M.L., Stein, P., Carvacho, I., Krapp, C., Ardestani, G., Mehregan, A., Umbach, D.M., Bartolomei, M.S., Fissore, R.A., and Williams, C.J. (2018). TRPM7 and Ca V3.2 channels mediate Ca 2+influx required for egg activation at fertilization. Proc. Natl. Acad. Sci. U S A *115*, E10370–E10378.

Calap-Quintana, P., González-Fernández, J., Sebastiá-Ortega, N., Llorens, V.J., and Moltó, D.M. (2017). *Drosophila melanogaster* models of metal-related human diseases and metal toxicity. Int. J. Mol. Sci. *18*, 1456.

Caldamone, A.A., Freytag, M.K., Cockett, A.T.K., and Cockett, T.K. (1979). Seminal zinc and male infertility. Urology *13*, 280–281.

Carlson, A.E. (2019). Mechanical stimulation activates *Drosophila* eggs via Trpm channels. Proc. Natl. Acad. Sci. U S A *116*, 18757–18758.

Cavaliere, V., Taddei, C., and Gargiulo, G. (1998). Apoptosis of nurse cells at the late stages of oogenesis of *Drosophila melanogaster*. Dev. Genes Evol. *208*, 106–112.

Cui, J., Sackton, K.L., Horner, V.L., Kumar, K.E., and Wolfner, M.F. (2008). Wispy, the *Drosophila* homolog of GLD-2, is required during oogenesis and egg activation. Genetics *178*, 2017–2029.

Duncan, F.E., Que, E.L., Zhang, N., Feinberg, E.C., O'Halloran, T.V., and Woodruff, T.K. (2016). The zinc spark is an inorganic signature of human egg activation. Sci. Rep. *6*, 24737.

Egli, D., Selvaraj, A., Yepiskoposyan, H., Zhang, B., Hafen, E., Georgiev, O., and Schaffner, W. (2003). Knockout of 'metal-responsive transcription factor' MTF-1 in *Drosophila* by homologous recombination reveals its central role in heavy metal homeostasis. EMBO J. *22*, 100–108.

Frassinetti, S., Bronzetti, G., Caltavuturo, L., Cini, M., and Croce, C. Della (2006). The role of zinc in life: a review. J. Environ. Pathol. Toxicol. Oncol. *25*, 597–610.

Gilston, B.A., Wang, S., Marcus, M.D., Canalizo-Hernandez, M.A., Swindell, E.P., Xue, Y., Mondragon, A., and O'Halloran, T.V. (2014). Structural and mechanistic basis of zinc regulation across the E. coli Zur regulon. Plos Biol. *12*, e1001987.

Heifetz, Y., Yu, J., and Wolfner, M.F. (2001). Ovulation triggers activation of *Drosophila* oocytes. Dev. Biol. *234*, 416–424.

Hester, J., Hanna-Rose, W., and Diaz, F. (2017). Zinc deficiency reduces fertility in *C. elegans* hermaphrodites and disrupts oogenesis and meiotic progression. Comp. Biochem. Physiol. C Toxicol. Pharmacol. *191*, 203–209.

Horner, V.L., Czank, A., Jang, J.K., Singh, N., Williams, B.C., Puro, J., Kubli, E., Hanes, S.D., Mckim, K.S., Wolfner, M.F., and Goldberg, M.L. (2006). The *Drosophila* calcipressin sarah is required for several aspects of egg activation. Med. Eng. Phys. *16*, 1441–1446.

Horner, V.L., and Wolfner, M.F. (2008a). Transitioning from egg to embryo: triggers and mechanisms of egg activation. Dev. Dyn. *237*, 527–544.

Horner, V.L., and Wolfner, M.F. (2008b). Mechanical stimulation by osmotic and hydrostatic pressure activates *Drosophila* oocytes in vitro in a calcium-dependent manner. Dev. Biol. *316*, 100–109.

Hu, Q., and Wolfner, M.F. (2019). The *Drosophila* Trpm channel mediates calcium influx during egg activation. Proc. Natl. Acad. Sci. U S A *116*, 18994–19000.

Kaneuchi, T., Sartain, C.V., Takeo, S., Horner, V.L., Buehner, N.A., Aigaki, T., and Wolfner, M.F. (2015). Calcium waves occur as *Drosophila* oocytes activate. Proc. Natl. Acad. Sci. U S A *112*, 791–796.

Kashir, J., Nomikos, M., Lai, F.A., and Swann, K. (2014). Sperm-induced Ca2+ release during egg activation in mammals. Biochem. Biophys. Res. Commun. *450*, 1204–1211.

Kim, A.M., Bernhardt, M.L., Kong, B.Y., Ahn, R.W., Vogt, S., Woodruff, T.K., and Halloran, T.V.O. (2011). Zinc sparks are triggered by fertilization and facilitate cell cycle resumption in mammalian eggs. ACS Chem. Biol. *6*, 716–723.

Kim, A.M., Vogt, S., O'Halloran, T.V., and Woodruff, T.K. (2010). Zinc availability regulates exit from meiosis in maturing mammalian oocytes. Nat. Chem. Biol. *6*, 674–681.

Knapp, E., and Sun, J. (2017). Steroid signaling in mature follicles is important for *Drosophila* ovulation. Proc. Natl. Acad. Sci. U S A *114*, 699–704.

Kong, B.Y., Duncan, F.E., Que, E.L., Kim, A.M., O'Halloran, T.V., and Woodruff, T.K. (2014). Maternally-derived zinc transporters ZIP6 and ZIP10 drive the mammalian oocyte-to-egg transition. Mol. Hum. Reprod. *20*, 1077–1089.

Kong, B.Y., Duncan, F.E., Que, E.L., Xu, Y., Vogt, S., O'Halloran, T.V., and Woodruff, T.K. (2015). The inorganic anatomy of the mammalian preimplantation embryo and the requirement of zinc during the first mitotic divisions. Dev. Dyn. *244*, 935–947.

Krauchunas, A.R., Sackton, K.L., and Wolfner, M.F. (2013). Phospho-regulation pathways during egg activation in *Drosophila melanogaster*. Genetics *195*, 171–180.

Kvist, U., Björndahl, L., and Kjellberg, S. (1987). Sperm nuclear zinc, chromatin stability, and male fertility. Scanning Microsc. *1*, 1241–1247.

Leader, D.P., Krause, S.A., Pandit, A., Davies, S.A., and Dow, J.A.T. (2017). FlyAtlas 2: a new version of the *Drosophila melanogaster* expression atlas with RNA-Seq, miRNA-Seq and sex-specific data. Nucleic Acids Res. *46*, D809–D815.

McLaughlin, J.M., and Bratu, D.P. (2015). *Drosophila melanogaster* oogenesis: an overview. In *Drosophila* Oogenesis: Methods and Protocols, D.P. Bratu and G.P. McNeil, eds. (Springer New York), pp. 1–20.

Mendoza, A.D., Woodruff, T.K., Wignall, S.M., and O'Halloran, T.V. (2017). Zinc availability during germline development impacts embryo viability in *Caenorhabditis elegans*. Comp. Biochem. Physiol. C Toxicol. Pharmacol. *191*, 194–202.

Mochida, S., and Hunt, T. (2007). Calcineurin is required to release *Xenopus* egg extracts from meiotic M phase. Nature *449*, 336–340.

Page, A.W., and Orr-Weaver, T.L. (1997). Activation of the meiotic divisions in *Drosophila* oocytes. Dev. Biol. *183*, 195–207.

Pepling, M.E., and Spradling, A.C. (2001). Mouse ovarian germ cell cysts undergo programmed breakdown to form primordial follicles. Dev. Biol. *234*, 339–351.

Percival, S.S., and Layden-Patrice, M. (1992). HL-60 cells can be made copper deficient by incubating with tetraethylenepentamine. J. Nutr. *122*, 2424–2429.

Que, E.L., Bleher, R., Duncan, F.E., Kong, B.Y., Gleber, S.C., Vogt, S., Chen, S., Garwin, S.A., Bayer, A.R., Dravid, V.P., et al. (2015). Quantitative mapping of zinc fluxes in the mammalian egg reveals the origin of fertilization-induced zinc sparks. Nat. Chem. *7*, 130–139.

Que, E.L., Duncan, F.E., Bayer, A.R., Philips, S.J., Roth, E.W., Bleher, R., Gleber, S.C., Vogt, S., Woodruff, T.K., O'Halloran, T.V., et al. (2017). Zinc sparks induce physiochemical changes in the egg zona pellucida that prevent polyspermy. Integr. Biol. *9*, 135–144.

Que, E.L., Duncan, F.E., Lee, H.C., Hornick, J.E., Vogt, S., Fissore, R.A., O'Halloran, T.V., and Woodruff, T.K. (2019). Bovine eggs release zinc in response to parthenogenetic and sperm-induced egg activation. Theriogenology *127*, 41–48.

Roohani, N., Hurrell, R., Kelishadi, R., and Schulin, R. (2013). Zinc and its importance for human health: an integrative review. J. Res. Med. Sci. *18*, 144–157.

Sartain, C.V., and Wolfner, M.F. (2013). Calcium and egg activation in *Drosophila*. Cell Calcium *53*, 10–15.

Schweigel-Röntgen, M. (2014). Chapter nine - the families of zinc (SLC30 and SLC39) and copper (SLC31) transporters. In Current Topics in Membranes, Exchangers, M. Bevensee, ed. (Academic Press), pp. 321–355.

Suzuki, T., Yoshida, N., Suzuki, E., Okuda, E., and Perry, A.C.F. (2010). Full-term mouse development by abolishing Zn2+-dependent metaphase II arrest without Ca2+ release. Development *137*, 2659–2669.

Swann, K., and Lai, F.A. (2016). Egg activation at fertilization by a soluble sperm protein. Physiol. Rev. *96*, 127–149.

Takeo, S., Hawley, R.S., and Aigaki, T. (2010). Calcineurin and its regulation by Sra/RCAN is required for completion of meiosis in *Drosophila*. Dev. Biol. *344*, 957–967.

Takeo, S., Tsuda, M., Akahori, S., Matsuo, T., and Aigaki, T. (2006). The calcineurin regulator sra plays an essential role in female meiosis in *Drosophila*. Med. Eng. Phys. *16*, 1435–1440.

Tejeda-Guzmán, C., Rosas-Arellano, A., Kroll, T., Webb, S.M., Barajas-Aceves, M., Osorio, B., and Missirlis, F. (2018). Biogenesis of zinc storage granules in *Drosophila melanogaster*. J. Exp. Biol. *221*, jeb168419.

Tian, X., Anthony, K., Neuberger, T., and Diaz, F.J. (2014). Preconception zinc deficiency disrupts postimplantation fetal and placental development in Mice1. Biol. Reprod. *90*, 83.

Tian, X., and Diaz, F.J. (2013). Acute dietary zinc deficiency before conception compromises oocyte epigenetic programming and disrupts embryonic development. Dev. Biol. *376*, 51–61.

Tian, X., and Diaz, F.J. (2012). Zinc depletion causes multiple defects in ovarian function during the periovulatory period in mice. Endocrinology *153*, 873–886.

Tokuhiro, K., and Dean, J. (2018). Glycan-independent gamete recognition triggers egg zinc sparks and ZP2 cleavage to prevent polyspermy. Dev. Cell *46*, 627–640.e5.

Tran, S.L., and Welte, M.A. (2010). In-vivo centrifugation of *Drosophila* embryos. J. Vis. Exp. *40*, 2005.

von Stetina, J.R., and Orr-Weaver, T.L. (2011). Developmental control of oocyte maturation and egg activation in metazoan models. Cold Spring Harb. Perspect. Biol. *3*, 1–19.

Yepiskoposyan, H., Egli, D., Fergestad, T., Selvaraj, A., Treiber, C., Multhaup, G., Georgiev, O., and Schaffner, W. (2006). Transcriptome response to heavy metal stress in *Drosophila* reveals a new zinc transporter that confers resistance to zinc. Nucleic Acids Res. *34*, 4866–4877.

York-Andersen, A.H., Parton, R.M., Bi, C.J., Bromley, C.L., Davis, I., and Weil, T.T. (2015). A single and rapid calcium wave at egg activation in *Drosophila*. Biol. Open *4*, 553–560.

Zhang, Z., Ahmed-Braimah, Y., Goldberg, M.L., and Wolfner, M.F. (2018). Calcineurin-dependent protein phosphorylation changes during egg activation in *Drosophila melanogaster*. Mol. Cell Proteomics *18*, S145–S158.

Zhang, N., Duncan, F.E., Que, E.L., O'Halloran, T.V., Woodruff, T.K., O'Halloran, T.V., and Woodruff, T.K. (2016). The fertilization-induced zinc spark is a novel biomarker of mouse embryo quality and early development. Sci. Rep. *6*, 22772.

iScience, Volume *23*

Supplemental Information

Zinc Dynamics during *Drosophila* Oocyte Maturation and Egg Activation

Qinan Hu, Francesca E. Duncan, Andrew B. Nowakowski, Olga A. Antipova, Teresa K. Woodruff, Thomas V. O'Halloran, and Mariana F. Wolfner

Transparent Methods

Fly strains and maintenance

All *Drosophila* strains and crosses were maintained or performed at 25 °C on a 12/12 light/dark cycle, on standard yeast-glucose-agar media (10% w/v yeast, 8.9% w/v agar (Genesee #66-111), 10% w/v glucose, 0.05% v/v phosphoric acid, 0.5% v/v propionic acid, 0.27% w/v p-hydroxybenzoic acid methyl ester, 2.5% v/v ethanol). When needed, 10 mM N,N,N′,N′-tetrakis(2-pyridiylmethyl)-1,2-ethylenediamine (TPEN) in ethanol, 10 mM neocuproine in ethanol, 10 mM ammonium tetrathiomolybdate (TM) in water or 10mM $ZnSO_4$ in water stock solution was added to melted food to the indicated final concentration and mixed well before the food solidified. An equal volume of solvent (ethanol or water) was added to control food. All chemicals were obtained from MilliporeSigma.

Egg-laying and egg hatchability assay

Oregon-R-P2 (ORP2) wildtype flies were reared on control yeast-glucose medium, or this medium containing the indicated concentrations of TPEN (TPEN food), or medium containing TPEN and $ZnSO_4$ (TPEN rescue food). To determine how TPEN affected fertility, 3- to 5-day-old virgin females and males were mated in single pairs on TPEN food. Matings were observed and the males were removed after a single mating had completed. Females were allowed to lay eggs in the mating vial for 24 hours and were then transferred to a new vial also containing TPEN food. Females were transferred twice to new vials of TPEN food before being discarded. The number of eggs and pupae in each vial were counted. Egg hatchability was calculated by dividing the number of pupae by the number of eggs. For 3 pairs of single matings from each group, we counted the number of unhatched eggs for two days after egg-laying to calculate the number of hatched ones. Those numbers were equal to the eventual number of pupae in the selected vials, confirming the reliability of our method of calculating egg hatchability. The same procedure was followed for assays with neocuproine and TM.

DNA constructs and transgenic flies

To create a null allele of *znt35C*, we generated pU6-chiRNA constructs following protocols described on the FlyCRISPR website (https://flycrispr.org/; Gratz et al., 2013). We generated two constructs to express sgRNAs with the following target sequences (PAM sequences are underlined): gRNA1, GGGCACGATGACAATGATCCCGG; gRNA2, GCAGATTTTCCAAGGCATCGAGG. These constructs were co-injected by Rainbow Transgenic Flies, Inc. into *nos-Cas9-attP2* embryos. We identified a chromosome carrying an edited *znt35C* gene, in which a 2 bp deletion (CCGGGATCATTGTCATCGTGCCC, deleted bases are underlined) in exon 3 caused by gRNA1 led to a frameshift in the coding sequence of Znt35C's transmembrane domains and a premature stop codon. Since this mutation is predicted to completely disrupt Znt35C's transmembrane domain, it is likely a null allele. We established a fly stock that carries the mutated allele, which we have named *znt35C*^{1}, over the CyO balancer chromosome (See crossing scheme in **Figure S10**).

X-ray fluorescence microscopy sample preparation

Oocytes were dissected in isolation buffer (IB) from the indicated female virgin flies aged on yeasted food for 3-5 days as described by (Page and Orr-Weaver, 1997). *In vitro* activated eggs were made by incubating dissected mature oocytes in Modified Robb's buffer (Hu and Wolfner, 2019) for 30 min. *In vivo* activated but unfertilized eggs were collected on a grape-juice agar plate from the indicated female flies after they had mated with spermless males (Boswell, 1985; Hu and Wolfner, 2019). We attempted to prepare oocytes for microscopy by standard methods of washing and mounting samples in standard protocol that used 100 mM ammonium acetate solution (Kim et al., 2010), but the oocytes lysed under these conditions. Alternatively, we washed oocytes and eggs with a high osmolarity buffer (400 mM sucrose) which prevents oocytes from activating (Horner and Wolfner, 2008b). Oocytes and eggs were then transferred by forceps to a 1µL drop of 400 mM

sucrose on an intact 5 mm × 5 mm silicon nitride window (Norcada). Samples were allowed to dry on a heated stage warmed to 37 °C and stored in a desiccating canister until used.

Synchrotron-based X-ray fluorescence microscopy

X-ray fluorescence microscopy (XFM) was performed at beamline 2-ID-E at the Advanced Photon Source (Argonne National Laboratory). With a single-bounce Si (111) monochromator, 10-keV X-rays were monochromatized and focused to a spot size of 1 × 1 μm using Fresnel-zone plate optics (X-radia). Raster scans were done in steps of 1 μm with 15° sample tilt to detector. Fluorescence spectra were collected with a 10 ms dwell time using a 4-element silicon drift detector (Vortex-EM). Quantification and image processing were performed with MAPS software (Vogt, 2003). The fluorescence signal was converted to a two-dimensional concentration in $\mu g/cm^2$ by fitting the spectra against the thin-film standard AXO 1X (AXO Dresden GmbH). We assumed that no elemental content was lost during sample preparation.

Statistics

One-way ANOVA tests were used to detect significant differences in levels of transition metals between wildtype and *znt35C*^{1} across oocyte stages and in egg number and egg hatchability upon TPEN, neocuproine, ammonium tetrathiomolybdate (TM) or $ZnSO_4$ treatment. Tukey's HSD test or Duncan's new multiple range test was used to identify groups that were significantly different from each other in the ANOVA tests.

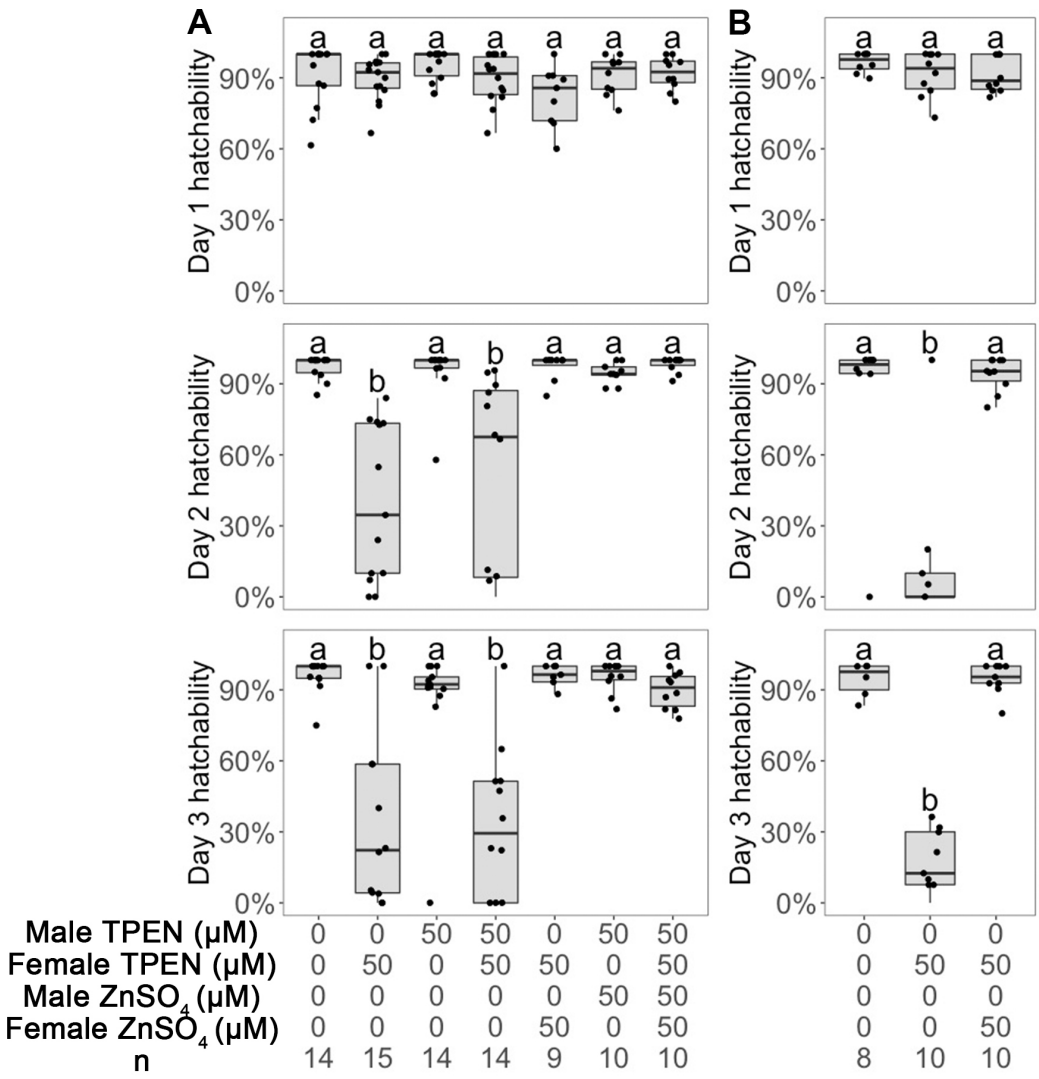

Figure S1 50 μM dietary TPEN reduces female *Drosophila* egg hatchability from day 2 post mating, related to Figure 1. (A) Egg hatchability breakdown by day of **Figure 1B**. 50 μM dietary TPEN significantly reduces females egg hatchability starting from day 2. **(B)** Egg hatchability of the second generation of females reared on TPEN mated with control males reared on normal food. Egg hatchability is still significantly reduced from day 2 post mating. Male TPEN: concentration of dietary TPEN on which the males were raised and tested. Female TPEN: concentration of TPEN added to food on which the females were raised and tested. Male $ZnSO_4$: concentration of $ZnSO_4$ added to food on which the males were raised. Female $ZnSO_4$: concentration of $ZnSO_4$ added to food on which the females were raised. n: sample size of each group. a, b: significance groups (significant difference of mean with $p<0.05$ between groups with different labels).

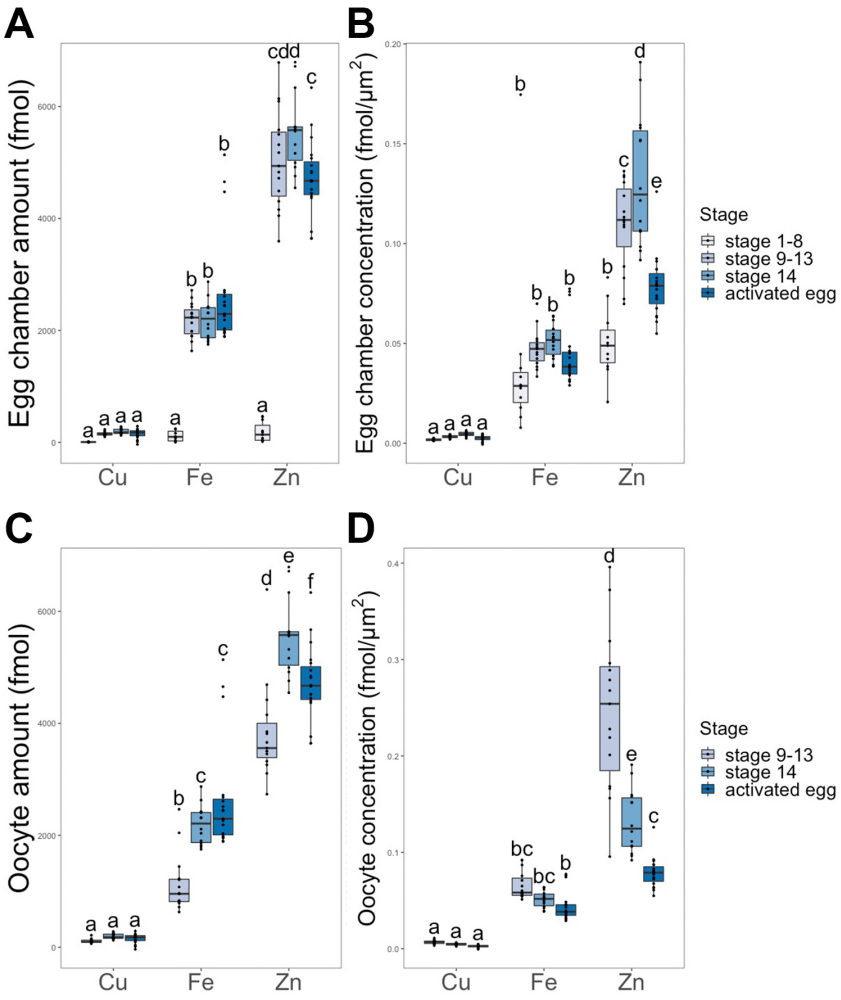

Figure S2 Levels of copper, iron and zinc in egg chambers and within oocytes during *Drosophila* oogenesis and egg activation, related to Figure 2. Copper, iron and zinc are the most abundant transition metals measured during oogenesis and egg activation. The total metal content **(A and C)** and metal concentration **(B and D)** in egg chambers **(A-B)** and oocytes **(C-D)** are plotted. Stage 1-8 oocytes n=11, stage 9-13 oocytes n=15, stage 14 oocytes n=14, activated eggs n=19. a, b, c, d, e, f: significance groups (significant difference of mean with $p<0.05$ between groups with different labels).

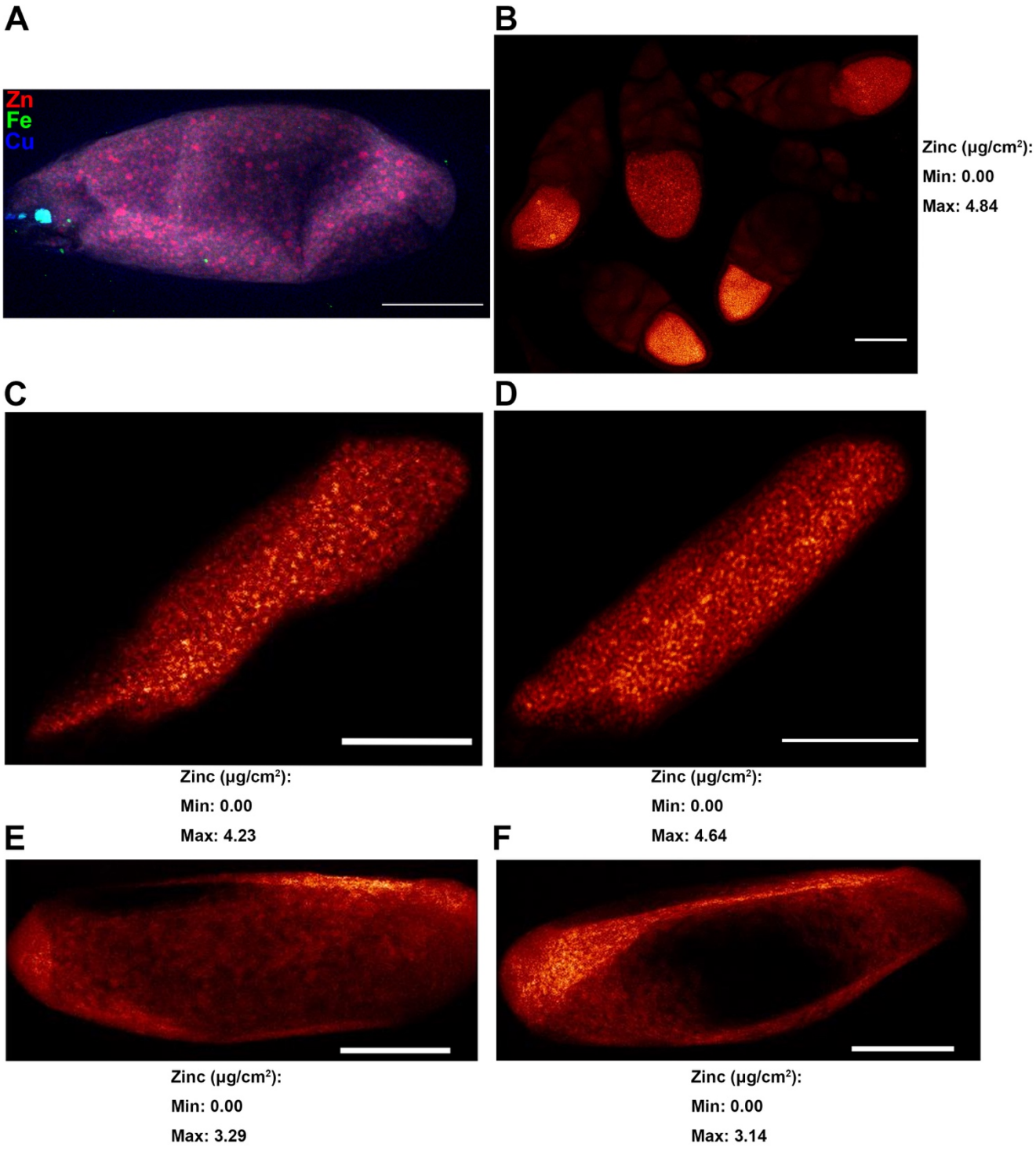

Figure S3 Additional examples of zinc distribution during oogenesis and after egg activation in wildtype *Drosophila*, related to Figure 3. (A) Overlay of iron, copper and zinc distribution in **Figure 3B**. Red: zinc, green: iron, blue: copper. **(B-F)**Representative XFM images showing zinc distribution in: **(B)** Egg chambers around stage 10; **(C-D)** Stage 14 mature oocytes; **(E-F)** Activated but unfertilized eggs. All scale bars = 100 µm.

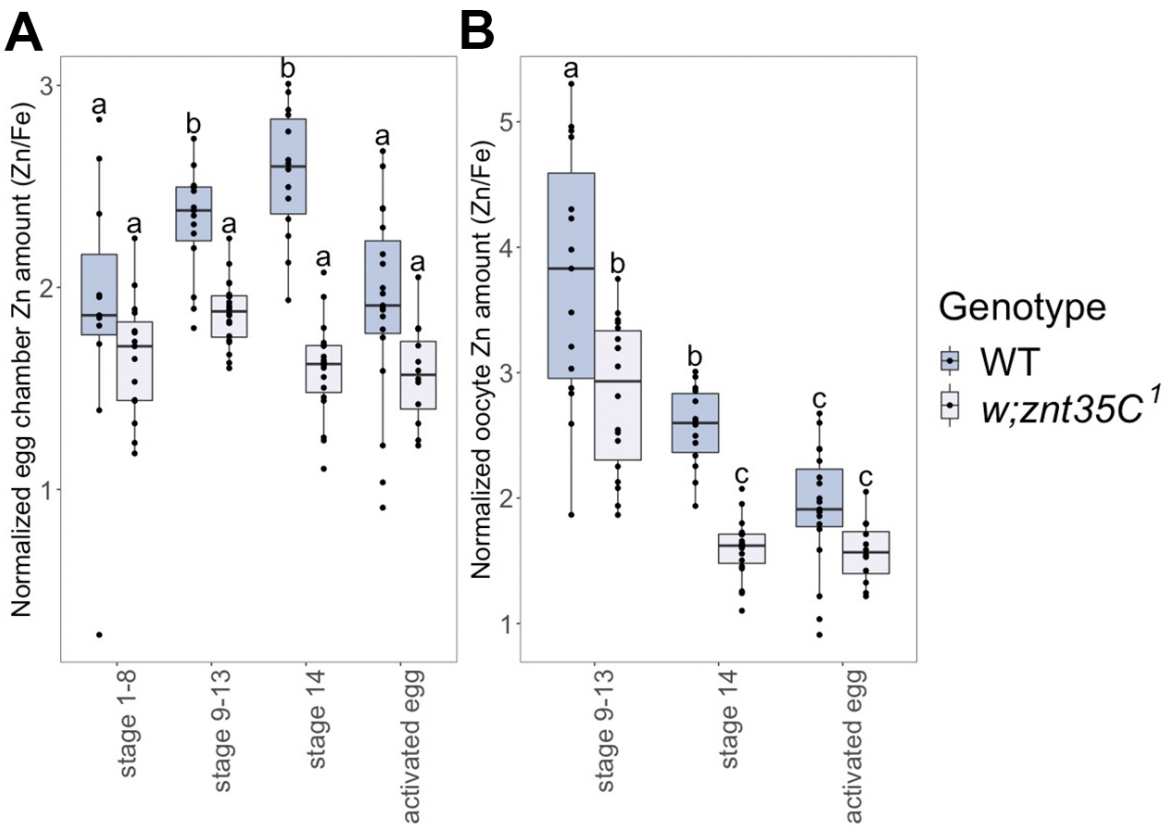

Figure S4 Normalized zinc quantification over oocyte maturation and activation in wildtype and *w; znt35C[1] Drosophila*, related to Figure 2. Zinc content normalized to iron content in ORP2 wildtype and *w; znt35C[1]* in each egg chamber **(A)** and **(B)** oocyte. WT: ORP2 wildtype. KO: *w; znt35C[1]* null mutant. Stage 1-8 oocytes WT n=11, KO n=15, stage 9-13 oocytes WT n=15, KO n =20, stage 14 oocytes WT n=14, KO n=19, activated eggs WT n=19, KO n=12. a, b, c: significance groups (significant difference of mean with $p<0.05$ between groups with different labels).

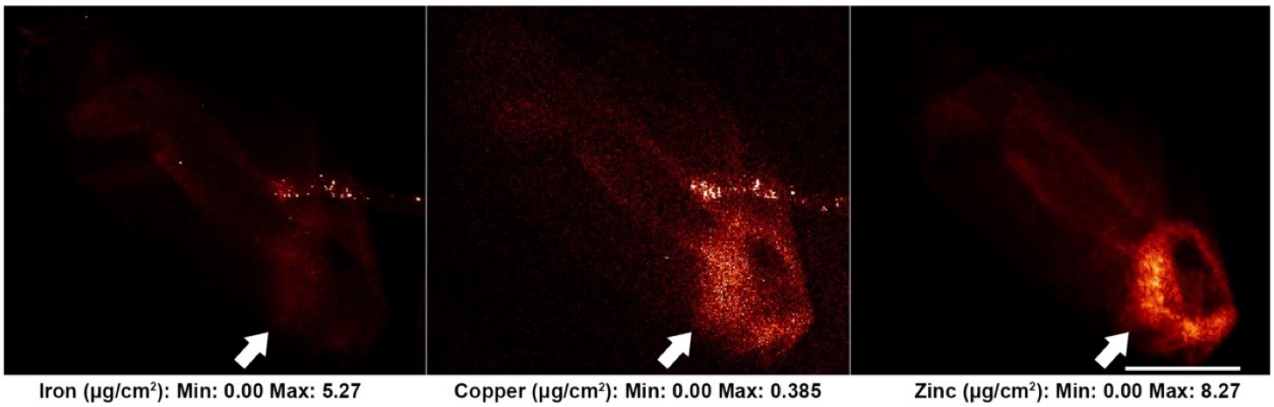

Figure S5 Distribution of iron, copper and zinc in centrifuged eggs activated *in vivo*, related to Figure 3. Iron, copper and zinc accumulated at the posterior end (indicated by arrows) of *in vivo* activated eggs after centrifugation (n=3). Scale bar = 100 µm.

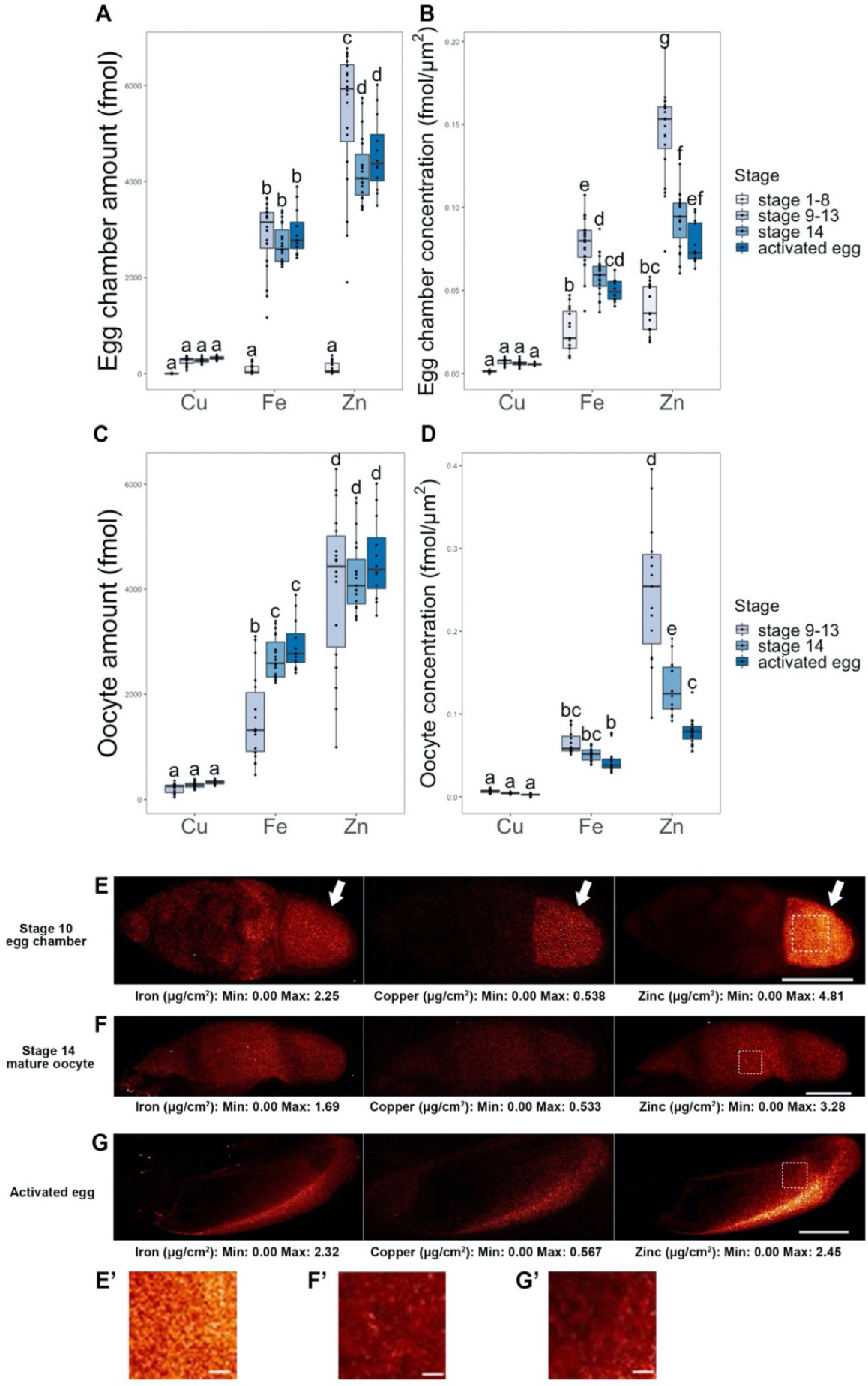
A
Egg chamber amount (fmol)
Cu
Fe
Zn
B
Egg chamber concentration (fmol/µm²)
Stage
stage 1-8
stage 9-13
stage 14
activated egg
C
Oocyte amount (fmol)
D
Oocyte concentration (fmol/µm²)
E
Stage 10
egg chamber
Iron (µg/cm²): Min: 0.00 Max: 2.25
Copper (µg/cm²): Min: 0.00 Max: 0.538
Zinc (µg/cm²): Min: 0.00 Max: 4.81
F
Stage 14
mature oocyte
Iron (µg/cm²): Min: 0.00 Max: 1.69
Copper (µg/cm²): Min: 0.00 Max: 0.533
Zinc (µg/cm²): Min: 0.00 Max: 3.28
G
Activated egg
Iron (µg/cm²): Min: 0.00 Max: 2.32
Copper (µg/cm²): Min: 0.00 Max: 0.567
Zinc (µg/cm²): Min: 0.00 Max: 2.45
E'
F'
G'

Figure S6 Levels and distributions of copper, iron and zinc in egg chambers and within oocytes during oogenesis and egg activation in *w; znt35C^{1}*, related to Figure 4. Copper, iron and zinc remain the most abundant transition metals measured during oogenesis and egg activation in *w; znt35C^{1}* mutants. The total metal content **(A and C)** and metal concentration **(B and D)** in egg chambers **(A-B)** and oocytes **(C-D)** are plotted. Stage 1-8 oocytes n=15, stage 9-13 oocytes n=20, stage 14 oocytes n=19, activated eggs n=12. a, b, c, d, e, f, g: significance groups (significant difference of mean with $p<0.05$ between groups with different labels). **(E-G)** In *w; znt35C^{1}* mutants, representative XFM images showing iron, copper and zinc distribution in: **(E)** an egg chamber around stage 10. Within an egg chamber, iron, copper and zinc are all still more concentrated in the oocyte (arrows); **(F)** a mature oocyte (stage 14). Zinc displays an even distribution.; **(G)** an activated but unfertilized egg. Zinc displays an even distribution. Scale bars = 100 μm. **(E'-G')** Enlarged view of zinc distribution in **(E-G)**. Dashed squares indicate enlarged regions. Scale bars = 10 μm.

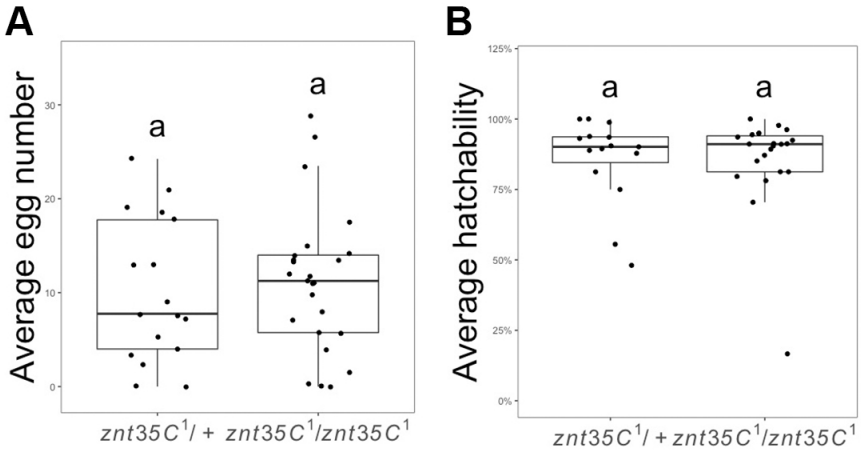

Figure S7 *znt35C[1]* does not affect female egg production and hatchability, related to Figure 4. Average **(A)** egg number and **(B)** hatchability over 4 days produced by control (*znt35C[1]*/+, n=17) and *znt35C* knockout (*znt35C[1]*/*znt35C[1]*, n=25) females mated with ORP2 wildtype males. a: significance groups (significant difference of mean with $p<0.05$ between groups with different labels).

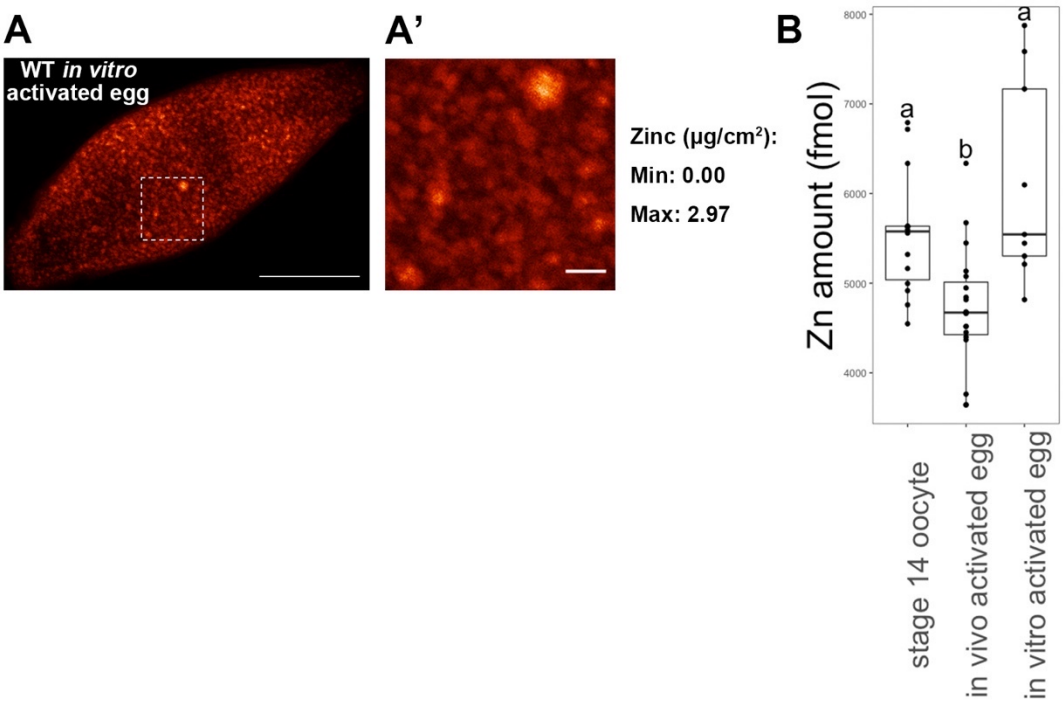

Figure S8 Zinc distribution and level in eggs activated *in* vitro, related to Figure 2 and 3. (A) Activation *in vitro* did not lead to a decrease in number of zinc-enriched granules in contrast to what was seen with *in vivo* egg activation. Scale bar = 100 µm; **(A')** Enlarged view of **(A)**. Dashed squares indicate enlarged regions. Scale bar = 10 µm; **(B)** Zinc levels in stage 14 mature oocyte, *in vivo* and *in vitro* activated eggs. Egg activation *in vitro* did not significantly reduce oocyte zinc levels in contrast to what was seen *in vivo* (stage 14 oocyte n=14, *in vivo* activated egg n=19, *in vitro* activated egg n=9). a, b: significance groups (significant difference of mean with $p<0.05$ between groups with different labels).

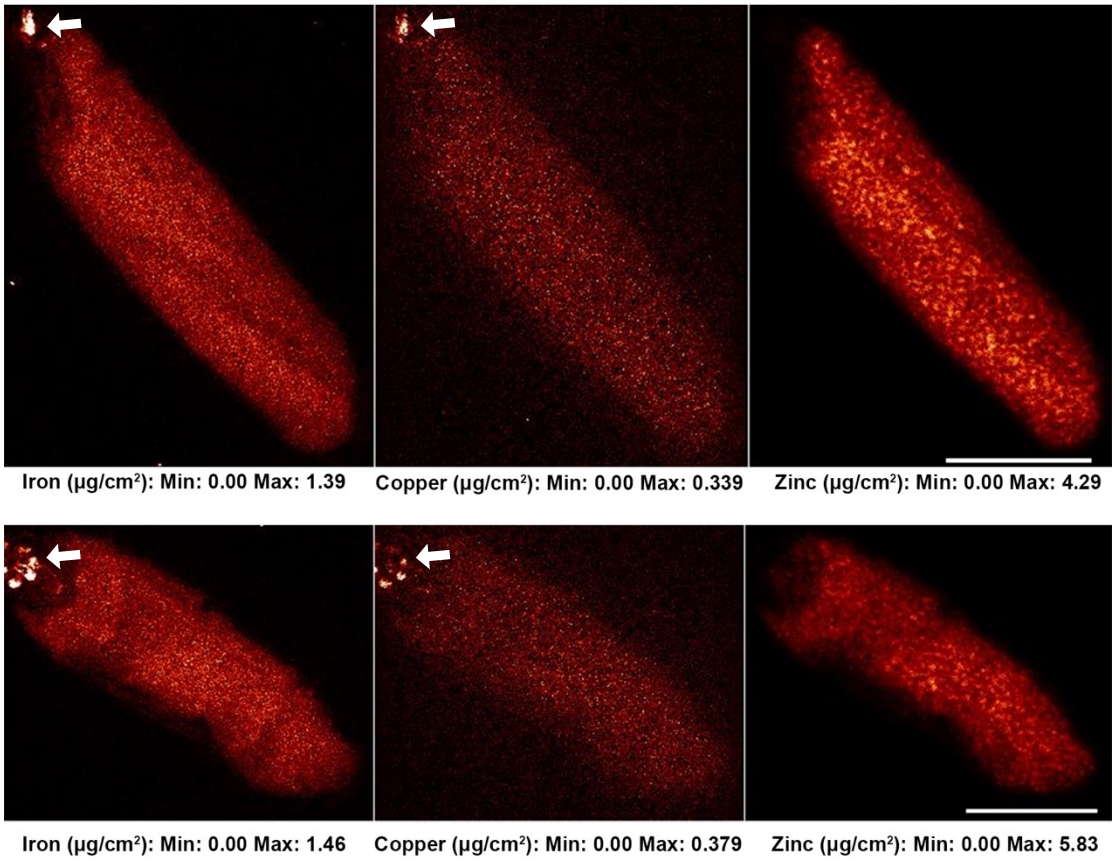

Figure S9 Additional examples showing granules enriched with iron and copper at the anterior end of wildtype mature oocytes, related to Figure 3. As seen in **Figure 3B**.

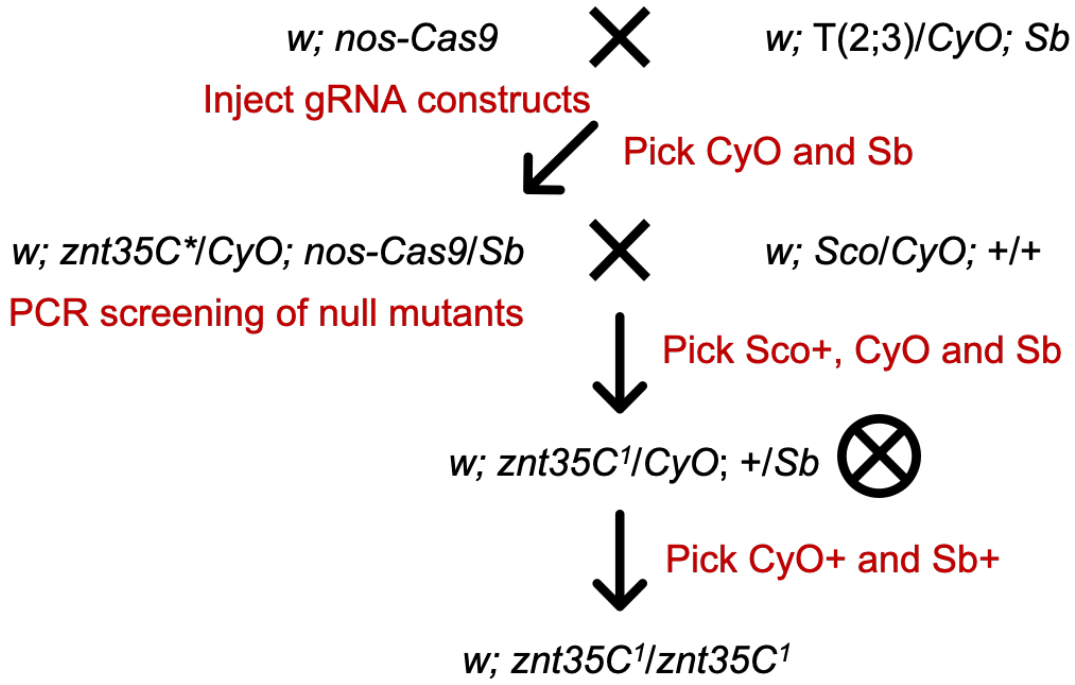

Figure S10 Crossing scheme to generate the *w; znt35C^{1}* mutant fly strain, related to Figure 4.